Integrating a Global CGE Model with a Terrestrial Nitrogen Flow Model for Assessing Climate Policy Impacts on Agriculture

Y. Osugi[1], K. Yamazaki[1], S. Fujimori[1], T. Hasegawa[2], K. Nishina[3]

[1]Department of Environmental Engineering, Kyoto University, Kyotodaigaku Katsura, Nishikyoku, Kyoto, Japan.

[2]Research Organization of Science and Technology, Ritsumeikan University, Kusatsu, Japan.

[3]Earth System Division, National Institute for Environmental Studies, Onogawa, Tsukuba, Japan.

Correspondence to: Y. Osugi (osugi.yuto.56n@st.kyoto-u.ac.jp)

Abstract

Human activities have caused an excess of reactive nitrogen in Earth systems, with increasingly apparent adverse effects on ecosystems and human health. Because the agriculture and land-use sector is a major source of reactive nitrogen, changes in land use and agricultural management strongly influence nitrogen flows, including inputs, gaseous emissions, and leaching. Evaluating how future changes in human activities and policy responses affect these flows requires linking integrated assessment models with process-based nitrogen flow models and assessing future nitrogen flows within an integrated framework. However, the Asia-Pacific Integrated Model framework lacks a module that represents terrestrial nitrogen flows at the grid scale. This study therefore developed a new grid-based terrestrial nitrogen flow model within this framework, examined its validity, and presented future nitrogen flows to provide a basis for discussing nitrogen-related issues under mitigation scenarios. The results show that the model estimated agricultural soil emissions of ammonia (NH3), nitrogen oxides (NOx), and nitrous oxide (N2O) for the base year 2010 at levels comparable to existing global emission inventories, indicating that it reproduces these emissions reasonably well at the global scale. By contrast, nitrogen leaching from agricultural land to soils and water bodies was estimated to be 5–46 Tg N yr-1 higher than in several previous studies. Given uncertainties in the parameters used to estimate nitrogen leaching in both this study and earlier work, as well as differences in estimation methods, this discrepancy does not appear to undermine model validity, although the leaching process could be improved through more detailed formulation. The framework developed in this study, including the terrestrial nitrogen flow model, provides a foundation for research on climate change, nitrogen cycling, atmospheric chemistry, and land use.

1. Introduction

Nitrogen is an essential element that constitutes nucleic acids, proteins, and other biomolecules, and is indispensable for the survival of all living organisms. Human activities have greatly increased the supply of reactive nitrogen (i.e., nitrogen compounds other than N_2), for example through biological nitrogen fixation and the production of synthetic fertilizers (Lassaletta et al., 2016). As a result, nitrogen inputs to cropland have increased rapidly since the twentieth century, supporting food production through increases in crop yields and food supply (Stewart and Roberts, 2012). At the same time, increases in nitrogen fixation and fertilizer application in agriculture, together with rising emissions of nitrogen oxides from other sectors, have led to a substantial increase in reactive nitrogen in terrestrial systems since the Industrial Revolution (Fowler et al., 2013).

Excess reactive nitrogen threatens global environmental sustainability through a wide range of environmental and human health impacts, including water pollution, air pollution, climate change, and biodiversity loss. Reactive nitrogen released from agricultural land contributes to eutrophication of aquatic systems, deterioration of air quality, and emissions of nitrous oxide (N_2O), a potent greenhouse gas. From this perspective, the Planetary Boundaries framework has proposed a boundary for biogeochemical nitrogen flows (De Vries et al., 2013), and it has been pointed out that current anthropogenic nitrogen fixation substantially exceeds this threshold (Galloway et al., 2003).

One of the major sources of reactive nitrogen responsible for these impacts is the agriculture and land-use sector. Synthetic fertilizers and livestock manure are the principal sources of nitrogen inputs to cropland. Part of these inputs is harvested in crops, whereas the remainder is released to the atmosphere as gaseous emissions or lost to soils, rivers, and groundwater. Lassaletta et al. (2016) reported that global cropland NUE declined markedly over the late twentieth century, implying that a large share of nitrogen inputs has been lost to the environment.

Future changes in human activities and policy responses may substantially alter the structure of the agriculture and land-use sector. Climate change mitigation, dietary change, livestock production systems, population growth, and advances in agricultural technology may affect cropland area, land-use patterns, crop yields, fertilizer demand, and livestock manure production (Popp et al., 2017). These changes in turn alter nitrogen flows such as fertilizer input, crop recovery, gaseous emissions, and leaching. Therefore, in evaluating the effects of diverse socioeconomic drivers, including climate change mitigation, on cropland nitrogen flows, it is important to capture not only greenhouse gas emissions but also changes in nitrogen flows induced by land-use change and crop yield change in an integrated manner.

To address this challenge, linking integrated assessment models that represent future scenarios of the economy, energy system, and land use with nitrogen flow models that explicitly describe nitrogen dynamics in cropland is highly useful. Existing emission inventories and many integrated assessment models estimate nitrogen emissions by multiplying country-level activity data by fixed emission factors (Crippa et al., 2018), which limits their ability to adequately reflect the effects of land-use change and improvements in fertilizer management on nitrogen flows. Previous studies have quantified cropland nitrogen budgets at the global scale, highlighted the importance of spatial heterogeneity, and examined long-term changes in nutrient surpluses (Smil, 1999; Liu et al., 2010; Bouwman et al., 2013). In addition, Beusen et al. (2022) linked an integrated assessment model with a nutrient model to assess nutrient loading under future socioeconomic scenarios. These studies provide important insights, but integrated assessment frameworks still often lack a module that can represent cropland nitrogen flows in a spatially explicit and process-based manner.

The Asia-Pacific Integrated Model (AIM) is a large family of integrated assessment models developed by multiple research institutions in the Asia-Pacific region, and it has been widely used for policy analysis of greenhouse gas mitigation and its impacts (Fujimori et al., 2017a). One of its core modules, the computable general equilibrium model AIM-Hub (Fujimori et al., 2017a), estimates nitrogen emissions by applying emission factors to activity levels by country and region. However, this framework alone makes it difficult to represent, in a process-based manner, the effects of climate change mitigation-induced land-use change and crop yield change on cropland nitrogen flows. Therefore, introducing into the AIM integrated assessment framework a nitrogen flow model that describes, at the grid scale, processes such as nitrogen inputs to cropland, crop uptake and recovery, gaseous emissions, and leaching to soils and water systems is an important step toward integrated evaluation of not only mitigation impacts but also multiple environmental objectives, including food, air quality, water quality, and biodiversity.

In this study, we develop a grid-based terrestrial nitrogen flow model within the AIM integrated assessment framework and examine its validity. We also present representative estimates of future terrestrial nitrogen flows using the constructed integrated assessment framework, thereby providing foundational information for discussing nitrogen-related issues under future scenarios, including climate change mitigation.

2. Methodology

2.1 General aspects

Figure 1a presents a schematic overview of the method used to calculate the nitrogen flow in this study. First, the computable general equilibrium model AIM-Hub[3)] estimates regionally aggregated land demand, synthetic fertilizer inputs, and anthropogenic emissions based on future scenarios. Next, the land-use allocation model AIM-PLUM[4)] uses the estimated land demand and land productivity as input data to determine land-use patterns. In addition, the atmospheric chemistry transport model GEOS-Chem[5)] estimates nitrogen deposition from the atmosphere using emission data and meteorological data as inputs. The emission data input to GEOS-Chem is downscaled from regional to 0.5° x 0.5° using a downscaling model called AIM-DS. Finally, the newly developed nitrogen flow model is used in this study to estimate each nitrogen flow in croplands (**Figure 1b**) on a 0.5° × 0.5° grid basis.

2.2 Nitrogen flow model

The nitrogen flow model calculates nitrogen flows in agricultural land on a grid basis (0.5° × 0.5°). This grid-based approach for estimating nitrogen flows at a 0.5° × 0.5° resolution has also been used in previous studies such as Bouwman et al. (2005). In the nitrogen budget model developed in this study, the nitrogen balance in agricultural land is broadly divided into inputs and losses.

The total nitrogen input to agricultural land includes the amount of nitrogen contained in synthetic fertilizer applied to agricultural land (IN_{fer}), the amount of nitrogen contained in manure and uncollected livestock excreta applied to agricultural land (IN_{man}), the amount of nitrogen deposited from the atmosphere to the soil (IN_{dep}), and the amount of nitrogen fixed in the soil through biological nitrogen fixation (IN_{fix}).

The total amount of nitrogen lost from agricultural land includes the amount of nitrogen contained in harvested crops and pasture consumed by livestock (OUT_{crop}), the amount of nitrogen contained in crop residues (OUT_{res}), the amount of nitrogen emitted to the atmosphere as NH_3, NO_x, N_2O, and N_2 (OUT_{gas}), and the amount of nitrogen leached from agricultural land to soils and water bodies (OUT_{lea}).

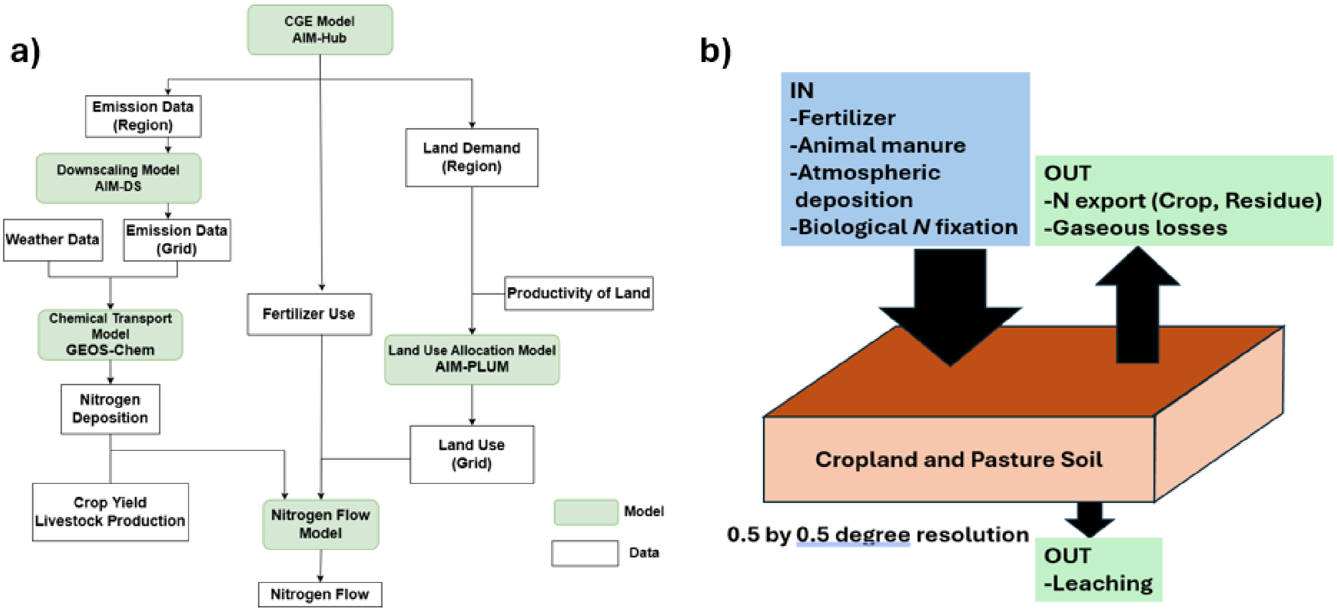

Figure 1 a) Overview of this study ; b) Main nitrogen flows in agricultural land represented by a nitrogen flow model

2.2.1 Fertilizer

The amount of nitrogen contained in synthetic fertilizer applied to agricultural land (IN_{fer}) is defined as the sum of the nitrogen contained in synthetic fertilizer applied to cropland (IN_{ferc}) and that applied to pastureland (IN_{ferp}) (Eq. (1)).

First, the amount of nitrogen applied as fertilizer estimated by AIM-Hub for each region (Table 1) was allocated into the portion applied to cropland ($fertc$) and the portion applied to pastureland ($fertp$) (Eq. (3) and (6)). Here, R denotes each region, y the target year, and sc the scenario. For this allocation, we used the shares of synthetic fertilizer applied to cropland (c) and to pastureland (p) from IFASTAT. The IFASTAT data used here contained missing values; following Nishina et al. (2017), these missing values were complemented using multiple imputation. For details of the multiple imputation method, see King et al. (2001). Next, IN_{ferc} was estimated by downscaling $fertc$ to the grid level as shown in Eq. (2), where lat and lon denote latitude and longitude, respectively. Likewise, IN_{ferp} was estimated by downscaling $fertp$ using the land-use fractions from AIM-PLUM output, as shown in Eq. (5).

$$IN_{fer}(lat, lon, y, sc) = IN_{ferc}(lat, lon, y, sc) + IN_{ferp}(lat, lon, y, sc) \quad (1)$$

$$IN_{ferc}(lat, lon, y, sc) = \sum_{sys} \left\{ fertc(R, y, sc) \cdot agrsys(sys) \cdot \frac{yieldgrid(lat, lon, y, sc, sys)}{\sum_{lon,lat} yieldgrid(R, lat, lon, y, sc, sys)} \right\} \quad (2)$$

$$fertc(R, y, sc) = fert(R, y, sc) \cdot c(R) \quad (3)$$

$$yieldgrid(lat, lon, y, sc, sys) = \sum_{crop} \left\{ yield(R, crop) \cdot \frac{LC(lat, lon, y, sc, sys, crop)}{\sum_{lon,lat} LC(R, lat, lon, y, sc, sys, crop)} \right\} \quad (4)$$

Regarding the classification of fertilizer inputs, following Liu et al. (2010), fertilizers are broadly divided into chemical fertilizers and other fertilizers. Chemical fertilizers are assumed to be applied to both irrigated and rainfed agriculture, whereas other fertilizers are assumed to be applied only to irrigated agriculture. In addition, using the global shares of chemical fertilizers and other fertilizers applied in 2015 (FAOSTAT), we calculated the share of chemical fertilizers applied to irrigated and rainfed agriculture, as well as the share of other fertilizers applied to irrigated agriculture ($agrsys$), where sys denotes the type of agricultural system. In this model, following a previous study (Tilman, 1999), crop yield is assumed to be linearly related to fertilizer input. Based on this assumption, the regionally estimated nitrogen input from synthetic fertilizer was downscaled with reference to the grid-based crop yield ($yieldgrid$), and the resulting value was defined as IN_{ferc}.

Next, we describe the method used to derive $yieldgrid$ from the regional crop yield ($yield$). First, FAOSTAT was used as the source of current production data. Country-level production data were then aggregated into the regional classification used in AIM-Hub (Table 1), and the target crops in GAEZ were aggregated into the crops to be estimated in the nitrogen budget model using the crop classification of AIM-PLUM. The resulting regional production data were then downscaled to the grid level using the land-use fractions from AIM-PLUM output, as shown in Eq. (4), where LC denotes the land use estimated by AIM-PLUM.

$$IN_{ferp}(lat, lon, y, sc) = \sum_{R} \left\{ fertp(R, y, sc) \cdot \frac{LC(lat, lon, y, sc)}{\sum_{lat,lon} LC(R, lat, lon, y, sc)} \right\} \tag{5}$$

$$fertp(R, y, sc) = fert(R, y, sc) \cdot p(R) \tag{6}$$

In addition, the temporal changes in synthetic fertilizer input for each scenario were represented by assuming that regional synthetic fertilizer input changes linearly with crop yield estimated by AIM-Hub. Furthermore, part of the crop residues that remain on agricultural land without being removed was assumed to be reused as synthetic fertilizer and was therefore included in IN_{fer} (Section 2.2.4).

2.2.2 Animal manure

The amount of nitrogen contained in manure applied to agricultural land (IN_{man}) is defined as the sum of the amount of nitrogen contained in manure applied to cropland (IN_{manc}) and the amount of nitrogen contained in manure and uncollected livestock excreta applied to pastureland (IN_{manp}) (Eq. (7)).

First, the method for estimating the amount of manure-derived nitrogen in agricultural land for each region is described. Livestock density by region in 2010, obtained from AIM-PLUM output, was multiplied by livestock-specific excretion rates (Bouwman et al., 1997) to estimate the amount of nitrogen contained in livestock excreta for each region. Next, the estimated amount of nitrogen in livestock excreta for each region was multiplied by the share of livestock produced in housing systems (Smil, 1999) to estimate the amount of nitrogen contained in collected excreta. Here, it was assumed that excreta are collected only in housing systems and are not collected on grazing land. Regarding losses occurring between excreta generation and collection and their application to agricultural land (e.g., collected manure that is not ultimately used), this study adopted a globally uniform value of 60%, following Smil (1999). Then, based on volatilization rates by manure management system (Hongmin et al., 2006), the fraction of nitrogen remaining in manure after volatilization was applied to estimate the amount of manure nitrogen that remains without volatilizing.

Furthermore, manure was allocated to cropland and pastureland based on the shares applied in developed and developing countries (Liu et al., 2010), yielding the amount of manure-derived nitrogen in cropland for each region ($Manurec$) and the amount of manure-derived nitrogen in pastureland for each region. Here, the share of manure applied to cropland was set to 66% in developed countries and 90% in developing countries, following Liu et al. (2010). In addition, the amount of nitrogen contained in uncollected excreta was added to the regional amount of manure-derived nitrogen in pastureland to obtain $Manurep$. In estimating the amount of nitrogen contained in uncollected excreta, the share of livestock produced on grazing land and the fraction remaining after volatilization (Smil, 1999) were used.

$$IN_{man}(lon, lat, y, sc) = IN_{manc}(lon, lat, y, sc) + IN_{manp}(lon, lat, y, sc) \tag{7}$$

$$IN_{manc}(lon, lat, y, sc) = Manurec(R, y, sc) \cdot \frac{LC(R, lon, lat, y, sc)}{\sum_{lon,lat} LC(R, lon, lat, y, sc)} \tag{8}$$

$$IN_{manp}(lon, lat, y, sc) = Manurep(R, y, sc) \cdot \frac{LC(R, lon, lat, y, sc)}{\sum_{lon,lat} LC(R, lon, lat, y, sc)} \tag{9}$$

IN_{manc} and IN_{manp} were obtained by downscaling the regional amounts of nitrogen contained in applied manure and uncollected livestock excreta to cropland and pastureland, respectively, using the land-use fractions from AIM-PLUM output, as shown in Eqs. (8) and (9). In addition, temporal changes by scenario were represented by assuming that the regional amount of manure changes linearly with livestock production estimated by AIM-Hub.

2.2.3 Other nitrogen inputs

The amount of nitrogen deposited from the atmosphere to agricultural land (IN_{dep}) was estimated by multiplying the output of the atmospheric chemical transport model GEOS-Chem (described later), representing total nitrogen deposition in each grid, by the land-use fraction of agricultural land in each grid. Both dry deposition and wet deposition were considered as forms of nitrogen deposition. In this study, although the specified scenarios account for changes in land use and nitrogen flows, the inputs to the terrestrial nitrogen flow model were based on GEOS-Chem output that does not reflect these changes.

The amount of nitrogen fixed in the soil through biological nitrogen fixation (IN_{fix}) was estimated by multiplying the agricultural land area in each grid by crop-specific coefficients representing the amount of fixed nitrogen: 60 kg N ha-1 for oil crops, 25 kg N ha-1 for irrigated paddy rice, 12 kg N ha-1 for other crops, and 5 kg N ha-1 for pastureland (Smil, 1999).

2.2.4 Nitrogen losses

This section describes the method used to estimate nitrogen losses from agricultural land. The amount of nitrogen emitted to the atmosphere as NH_3, NO_x, and N_2O (OUT_{gas}) was estimated by applying the regression equation used in Lesschen et al. (2004) (Eq. (10)) to each grid. Annual precipitation (P) was taken from The Modern-Era Retrospective analysis for Research and Applications Version 2 (MERRA-2) (Bosilovich et al., 2015). The amount of nitrogen contained in fertilizer applied to agricultural land (F) was defined as the sum of IN_fer and IN_man calculated in Sections b) and c). For soil organic carbon content (O), the baseline grid data from Sanderman et al. (2020) were used. The first part of Eq. (10) (inside the parentheses) represents emissions of NO_x and N_2O, while the second part represents NH_3 emissions. In addition, the emissions of NO_x, N_2O, and N_2 were calculated based on the ratios of NO_x, N_2O, and N_2 emitted from agricultural land (Smil, 1999; Stehfest and Bouwman, 2006).

$$OUT_{gas} = (0.025 + 0.000855 \times P + 0.01725 \times O) + 0.113 \times F \tag{10}$$

The amount of nitrogen contained in harvested crops and pasture consumed by livestock (OUT_{crop}) is defined as the sum of the amount of nitrogen contained in crops harvested from cropland and the amount of nitrogen contained in pasture harvested from pastureland and consumed by livestock.

The amount of nitrogen contained in crops harvested from cropland was estimated by multiplying the grid-based crop yield ($yieldgrid$), which was also used in the estimation of IN_{fer}, by the nitrogen content for each crop type. A globally uniform value was used for the nitrogen content of each crop. These values were estimated by taking the values provided by FAOSTAT and aggregating the target crops in GAEZ into the crop categories used for production estimation in the nitrogen budget model according to the AIM-PLUM crop classification, with weighting based on the production volume of each crop.

The amount of nitrogen contained in pasture harvested from pastureland and consumed by livestock was set, following Bouwman et al. (2005), to 0.6 times the value obtained by subtracting OUT_{gas} from total inputs for pastureland. This factor of 0.6 was based on the nitrogen recovery efficiency of pasture.

Next, the method used to estimate the amount of nitrogen contained in removed crop residues (OUT_{res}) is described. First, the amount of crop residues in each grid was obtained by multiplying the grid-based crop yield estimated above by the residue-to-product ratio (Milbrandt et al., 2005). The amount of nitrogen contained in crop residues was then estimated by multiplying the resulting crop residue amount by the nitrogen content for each crop type. As with the estimation of nitrogen content in crop production, the nitrogen content of crop residues was estimated using values provided by FAOSTAT, by aggregating the target crops in GAEZ into the crop categories used for production estimation in the nitrogen budget model according to the AIM-PLUM crop classification, with weighting based on the production volume of each crop. The removal rate of crop residues was set to 35% for developed countries and 50% for developing countries(Smil, 1999). Here, crop residues that were not removed were assumed to be reused as synthetic fertilizer and were therefore included in IN_{fer}. In addition, OUT_{res} was set to 0 for pastureland.

The amount of nitrogen leached from agricultural land to soils and water bodies (OUT_{lea}) was defined as the value obtained by subtracting OUT_{crop}, OUT_{res}, and OUT_{gas} from total inputs (Eq. (11)). In addition, this model does not consider water transport between grids.

$$OUT_{lea} = IN - (OUT_{crop} + OUT_{res} + OUT_{gas}) \tag{11}$$

2.3 Downscaling regional emissions

AIM-DS (Fujimori et al., 2017b) is a downscaling model that allocates regionally estimated emissions from AIM-Hub to a grid basis (0.5° × 0.5°). In AIM-DS, the downscaling algorithms are defined by sector and are broadly classified into three groups: Group 1 corresponds to industry, land transport, and residential/commercial sectors; Group 2 corresponds to energy, solvents, waste, agriculture, and related sectors; and Group 3 corresponds to shipping and aviation.

Group 1 uses GDP and population (Gridded Population of the World: GPW) as the drivers for downscaling. Emissions are downscaled on the basis of the downscaled GDP and population. In Group 2, the driver is the area of the emission source. In this study, for Group 2 sectors other than agriculture, the spatial pattern from CEDS for 2005 (Hoesly et al., 2018) is used for downscaling. Group 3 uses essentially the same basic algorithm as Group 2, but downscaling is conducted without considering regional boundaries.

2.4 Simulation of nitrogen deposition

GEOS-Chem is a chemical transport model (CTM) developed primarily by Harvard University. GEOS-Chem estimates atmospheric pollutant concentrations using input data such as meteorological conditions, emissions, atmospheric chemical concentrations, and reaction rate coefficients. It divides the globe into three-dimensional grid cells and simulates chemical reactions within each grid cell as well as the transport of chemical species between grid cells, thereby estimating atmospheric concentrations and deposition fluxes. For chemical reactions, GEOS-Chem considers detailed processes for more than 100 chemical species, including NO_x, VOCs, OH, and CH_4, and outputs variables such as atmospheric pollutant concentrations and radiative forcing by chemical species.

In this study, a globally uniform resolution of 4° × 5° was used, and the emission inventory was based on gridded emission data output from AIM-Hub. For other natural emission sources and reaction processes, the preset configurations were used. Meteorological data were taken from MERRA-2 (Bosilovich et al., 2015).

GEOS-Chem provides various simulation options depending on the target chemical species, chemical mechanisms, and vertical domain. The full-chemistry simulation is the most standard configuration, and it includes more than 100 chemical species, including nitrogen oxides, oxygen, bromine, chlorine, iodine, and aerosols. In the full-chemistry simulation, atmospheric pollutants such as NOx and VOCs (volatile organic compounds) are treated as emission inventories. In this study, the full-chemistry simulation was used to estimate the amount of reactive nitrogen deposited from the atmosphere.

2.5 Scenarios

In this study, in order to evaluate the impacts of climate change mitigation measures on land use, we assumed future scenarios combining emissions and socioeconomic pathways and estimated emissions under those scenarios. As emissions scenarios, we used a baseline scenario (Baseline) without explicit emissions constraints and a stringent climate change mitigation scenario (500C) that limits cumulative CO_2 emissions after 2018 to 500 Gt (Riahi et al., 2021). Hereafter, these are referred to as the Baseline and 500C scenarios, respectively. The analysis years were set to 2010, 2030, 2050, and 2100.

For the socioeconomic conditions, we adopted the Shared Socioeconomic Pathways (SSPs), which have been widely used in recent climate change research. The SSPs describe alternative future trajectories of socioeconomic development in terms of the challenges they pose for mitigation and adaptation. In this study, we used SSP2, a "middle-of-the-road" pathway, as the socioeconomic scenario.

3. Result

3.1 Model verification

Compared with existing inventories for nitrogen emissions from agricultural soils in 2010, the present model estimated lower NH3 emissions than EDGAR (Crippa et al., 2018) and a level broadly comparable to CEDS, whereas the differences in NO_x and N_2O emissions relative to AIM-Hub, FAOSTAT, and EDGAR were relatively small. Specifically, NH3 emissions from agricultural soils were approximately 6.9 Tg N yr^{-1} lower than those in EDGAR, and the combined total of NO_x and NH_3 was approximately 9.8 Tg N yr^{-1} lower than that in FAOSTAT. On the other hand, NH_3 emissions from agricultural soils in CEDS were almost the same as those estimated by the present model. Although the present model estimated somewhat higher NO_x and N_2O emissions than CEDS, the differences were comparable to those observed among the other inventories (**Table 1**). For the agricultural sector as a whole, the present model estimated NO_x and N_2O emissions to be approximately 1–2 Tg N yr^{-1} higher than those in the other emission inventories. In addition, NH_3 emissions were estimated to be about 13.4 Tg N yr^{-1} higher than AIM-Hub, 11.7 Tg N yr^{-1} higher than EDGAR, and 12.2 Tg N yr^{-1} higher than CEDS. Here, the agricultural sector as a whole includes not only emissions from agricultural soils but also nitrogen lost to the atmosphere from manure management systems (**Table 1**).

Regarding nitrogen leaching from agricultural land to soils and water bodies, the present model estimated a value of 62.7 Tg N yr^{-1} in 2010, which is higher than the range reported in previous studies (17.0–57.0 Tg N yr^{-1}). Although direct comparison is limited because the target years differ among studies, the estimate in this study exceeded the upper bound of previous estimates (**Table 2**).

A regional comparison of NH_3 emissions showed that, in both 2010 and 2020, China, India, and Europe had relatively large emissions in all four inventories. On the other hand, there were some differences in the relative magnitudes among inventories. In many regions, EDGAR showed the highest emissions, followed by AIM-Hub, whereas the estimates in this study were often similar to or slightly lower than those in CEDS. In contrast, in the United States and North Africa, the estimates in this study were sometimes comparable to or even higher than those in CEDS and AIM-Hub. Furthermore, in sub-Saharan Africa, EDGAR showed markedly higher emissions than the other inventories. Comparing 2010 and 2020, NH_3 emissions increased in many regions, including South America, China, and India, in all four inventories (**Figs. 2 and 3**).

Table 1 Comparison of nitrogen emissions from agricultural soils in 2010 (Tg N yr^{-1}) from the terrestrial nitrogen flow models in this study, AIM-Hub, FAOSTAT, and EDGAR

		NO_x	NH_3	N_2O
This study	Agricultural land soil	2.5	21	4.5
	Agricultural total	2.5	47	4.5
AIM-Hub	Agricultural land soil	1.0	25.9	3.9
	Agricultural total	1.1	35.0	4.1
EDGAR	Agricultural land soil	1.0	26.4	3.4
	Agricultural total	1.8	36.7	3.7
CEDS	Agricultural land soil	0.8	20.0	2.4
	Agricultural total	1.1	36.2	4.1
FAOSTAT	Agricultural land soil	31.8 (NO_x+NH_3)		3.8

Table 2 Comparison of nitrogen leaching from agricultural land to soils and water bodies in this study's terrestrial nitrogen flow model and in previous studies (Tg N yr-1)

	This Study	Smil et al. (1999)	Beusen et al. (2022)	Liu et al. (2010)	Bouwman et al. (2005)
Year	2010	1995	2015	2000	1995
Leaching	62.7	17.0	57.0	23.0	28.5

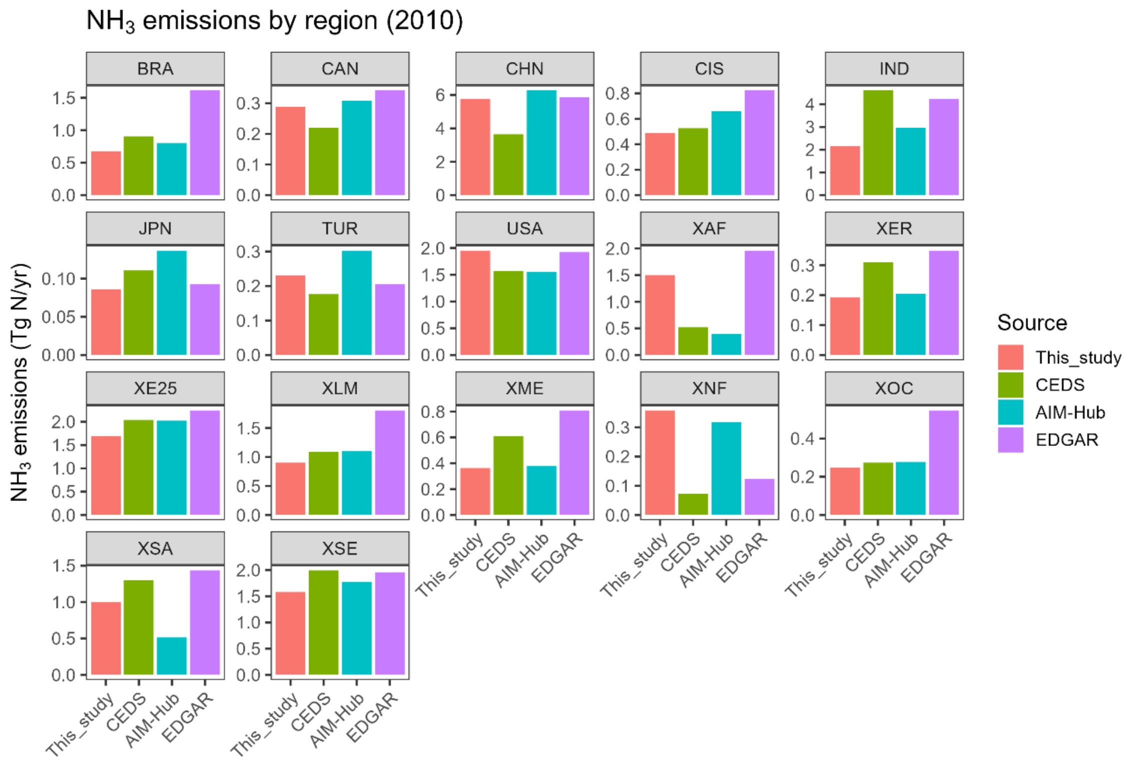

Figure 2 Regional comparison of agricultural soil NH_3 emissions in 2010 among the terrestrial nitrogen flow model developed in this study, AIM-Hub, EDGAR, and CEDS

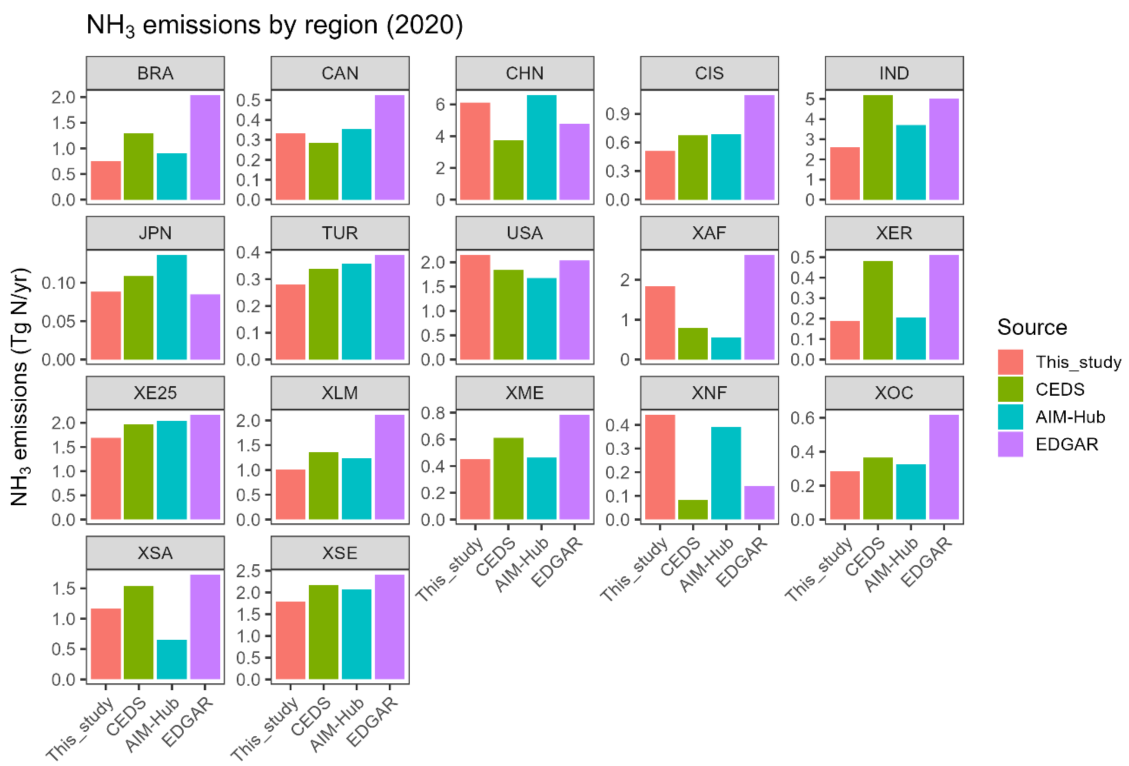

Figure 3 Regional comparison of agricultural soil NH_3 emissions in 2020 among the terrestrial nitrogen flow model developed in this study, AIM-Hub, EDGAR, and CEDS

3.2 Nitrogen flows in agricultural land

In future global agricultural land, both nitrogen inputs and outputs increase throughout the twenty-first century under both the Baseline and 500C scenarios, although the magnitude of the increase differs by scenario (**Fig. 4**). Under the Baseline scenario, IN_{fer} and IN_{man} increase substantially after 2030 compared with their 2010 levels. IN_{fer} reaches 148.9 Tg N yr^{-1} in 2030, 166.1 Tg N yr^{-1} in 2050, and 170.5 Tg N yr^{-1} in 2100. IN_{man} also increases in a similar manner, reaching 89.7 Tg N yr^{-1} in 2100. On the output side, OUT_{crop}, OUT_{gas}, OUT_{res}, and OUT_{lea} all increase over time, reaching 116.6 Tg N yr^{-1}, 53.8 Tg N yr^{-1}, 53.8 Tg N yr^{-1}, and 98.4 Tg N yr^{-1}, respectively, in 2100. It should be noted that the present model does not represent temporal changes in nitrogen stock in agricultural soils. Therefore, the reported nitrogen inputs and outputs should be interpreted as annual flows under a balanced-budget assumption, rather than as evidence of nitrogen accumulation or depletion in agricultural land.

Under the 500C scenario, the increase in IN_{man} after 2030 is smaller than in the Baseline scenario, reaching 56.5 Tg N yr^{-1} in 2030, 63.4 Tg N yr^{-1} in 2050, and 78.2 Tg N yr^{-1} in 2100. In addition, the increase in OUT_{lea} after 2030 is also smaller than in the Baseline scenario, reaching 65.4 Tg N yr^{-1} in 2030, 66.1 Tg N yr^{-1} in 2050, and 76.6 Tg N yr^{-1} in 2100.

Along with these changes, total nitrogen input to global agricultural land increases substantially after 2030, while nitrogen recovered as crops and crop residues (OUT_{crop} and OUT_{res}) also increases, leading to an improvement in nitrogen use efficiency (NUE) (**Fig. 4**). Thus, the reported inputs and outputs represent annual nitrogen flows and do not imply accumulation or depletion of nitrogen in agricultural land. Although this model does not explicitly specify a coefficient that directly determines the relationship between nitrogen input and crop yield, the resulting NUE in the Baseline scenario (defined as the share of inputs recovered as crops and crop residues) changes from 56.1% in 2010 to 56.6% in 2030, 56.0% in 2050, and 52.8% in 2100. Similarly, changes in NUE from the 2010 level are also observed under the 500C scenario, reaching 58.0% in 2030, 58.3% in 2050, and 55.0% in 2100, with NUE consistently higher than in the Baseline scenario at all time points.

Nitrogen inputs to agricultural land across the world's 17 regions differ greatly in both their absolute levels and future change patterns (**Figs. 5 and 7**). Under the Baseline scenario, total nitrogen input increases consistently from 2010 to 2100 in the United States, Canada, India, Brazil, and several other regions, whereas it remains at roughly constant levels in the EU25, the rest of Europe, and the former Soviet Union. In contrast, nitrogen input declines after 2010 in China and Japan, falling below the 2010 level by 2100. Looking at the components of nitrogen input, IN_{fer} accounts for the largest share in most regions, and future increases in total input are driven primarily by increases in IN_{fer} (**Fig. 5**). IN_{man} makes a relatively large contribution in regions with high livestock density, such as Brazil and sub-Saharan Africa, and increases over time. By contrast, IN_{dep} and IN_{fix} contribute only a small share of total input in most regions, and their temporal changes are also smaller than those of IN_{fer} and IN_{man}. Under the 500C scenario, the magnitude of increase over time is smaller in regions such as sub-Saharan Africa and Brazil (**Fig. 7**). However, the regional distribution of nitrogen inputs and the basic composition of their components do not differ substantially from those under the Baseline scenario.

Throughout the twenty-first century, nitrogen outputs from agricultural land increase in many regions, although their magnitude and temporal patterns vary considerably across regions (**Figs. 6 and 8**). Under the Baseline scenario, total nitrogen output increases consistently from 2010 to 2100 in the United States, Canada, India, Brazil, the rest of South America, the Middle East, and sub-Saharan Africa. In contrast, outputs remain at approximately constant levels throughout the century in the EU25, the rest of Europe, and the former Soviet Union. In China and Japan, total output remains nearly stable or declines slightly after 2010. Looking at the components of output, nitrogen removal through crop harvest (OUT_{crop}) is the largest contributor in all regions, and future increases in total output are driven primarily by increases in OUT_{crop} (**Fig. 6**). In the United States, Europe, and Japan, OUT_{res} makes a relatively large contribution and increases consistently over time. By contrast, in India, Canada, and the Middle East, OUT_{lea} contributes substantially, and by 2100 it becomes the largest flow among the outputs. Under the 500C scenario, the regional distribution and basic composition of nitrogen outputs from agricultural land are broadly similar to those under the Baseline scenario, although in regions such as sub-Saharan Africa and Canada, the share of OUT_{crop} in total output is higher than in the Baseline scenario (**Fig. 8**).

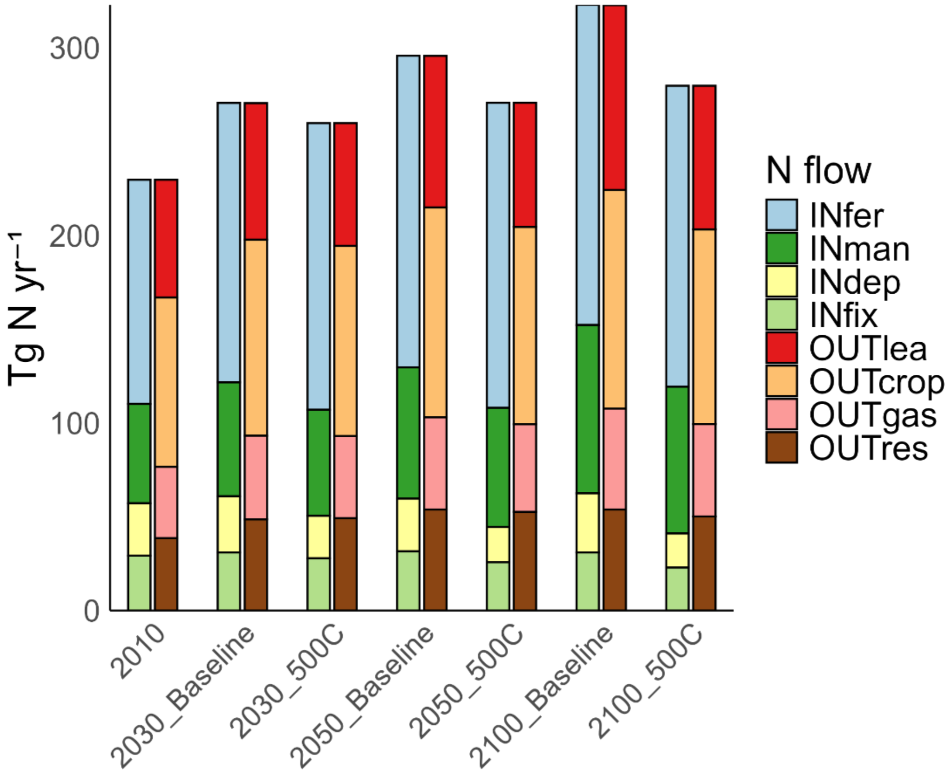

Figure 4 Nitrogen flows in the Baseline and 500C scenarios

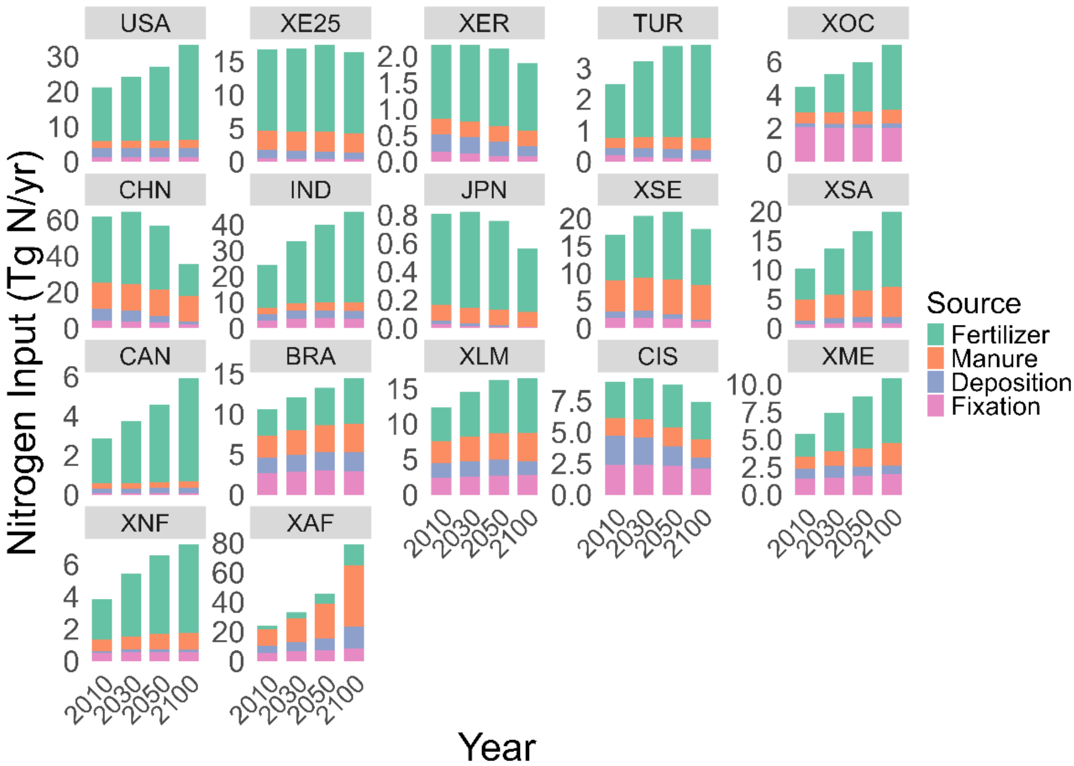

Figure 5 Temporal changes in nitrogen inputs to agricultural land by region (Baseline)

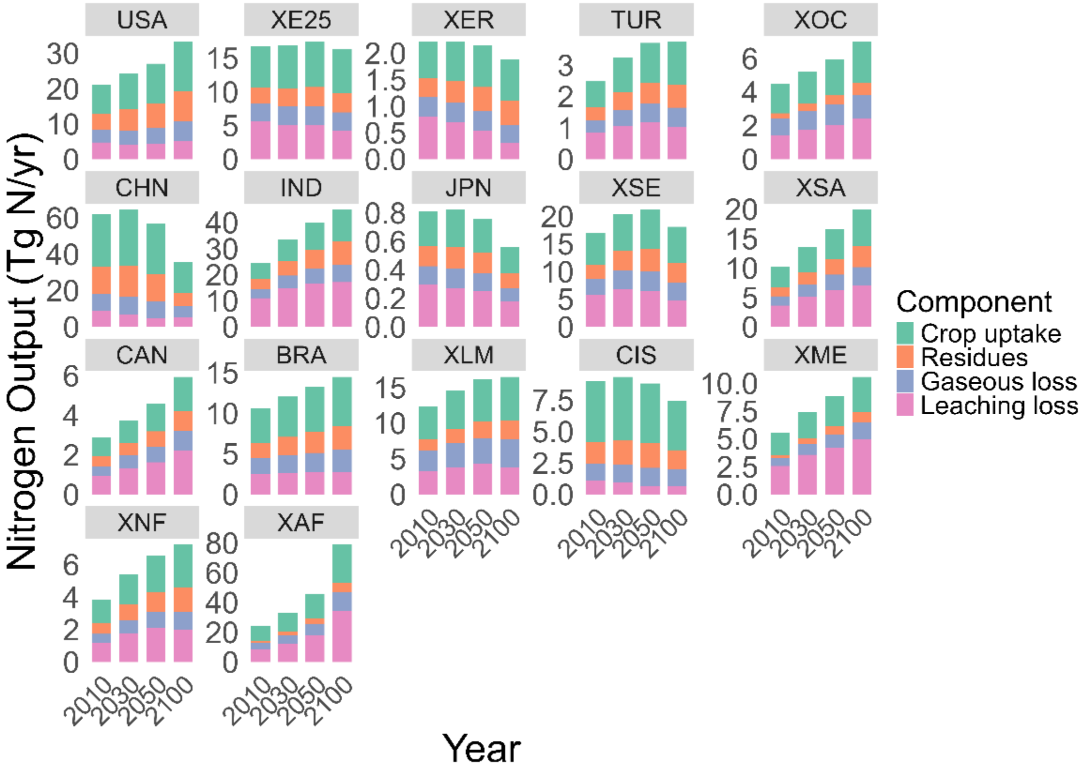

Figure 6 Temporal changes in nitrogen outputs from agricultural land by region (Baseline)

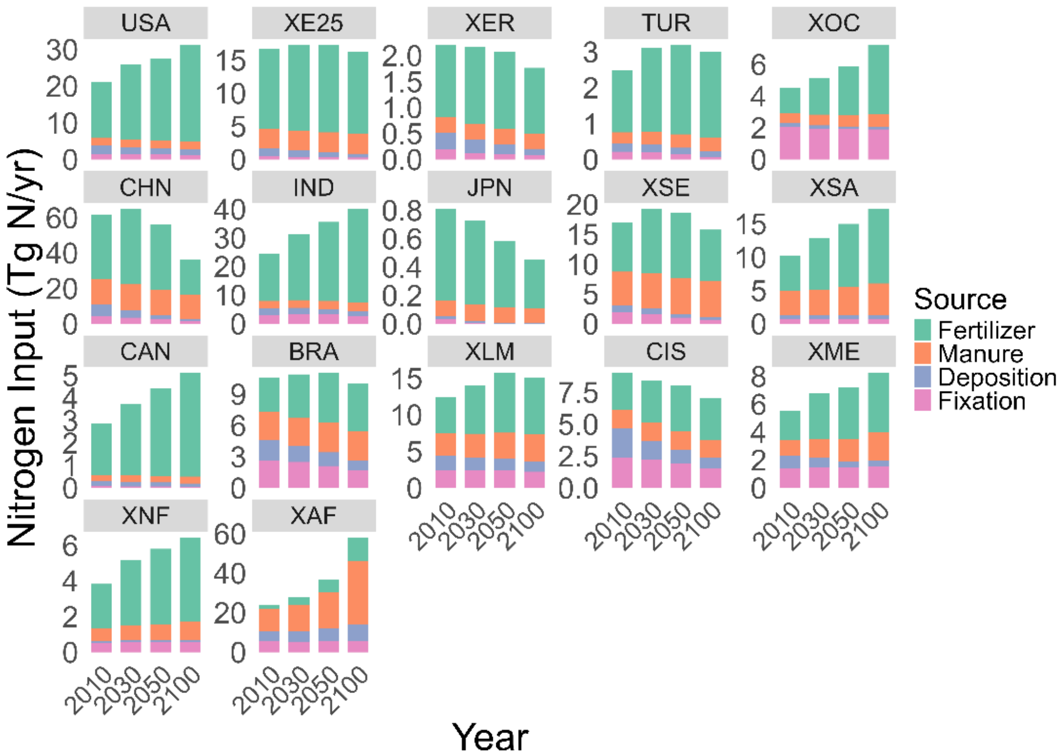

Figure 7 Temporal changes in nitrogen inputs to agricultural land by region (500C)

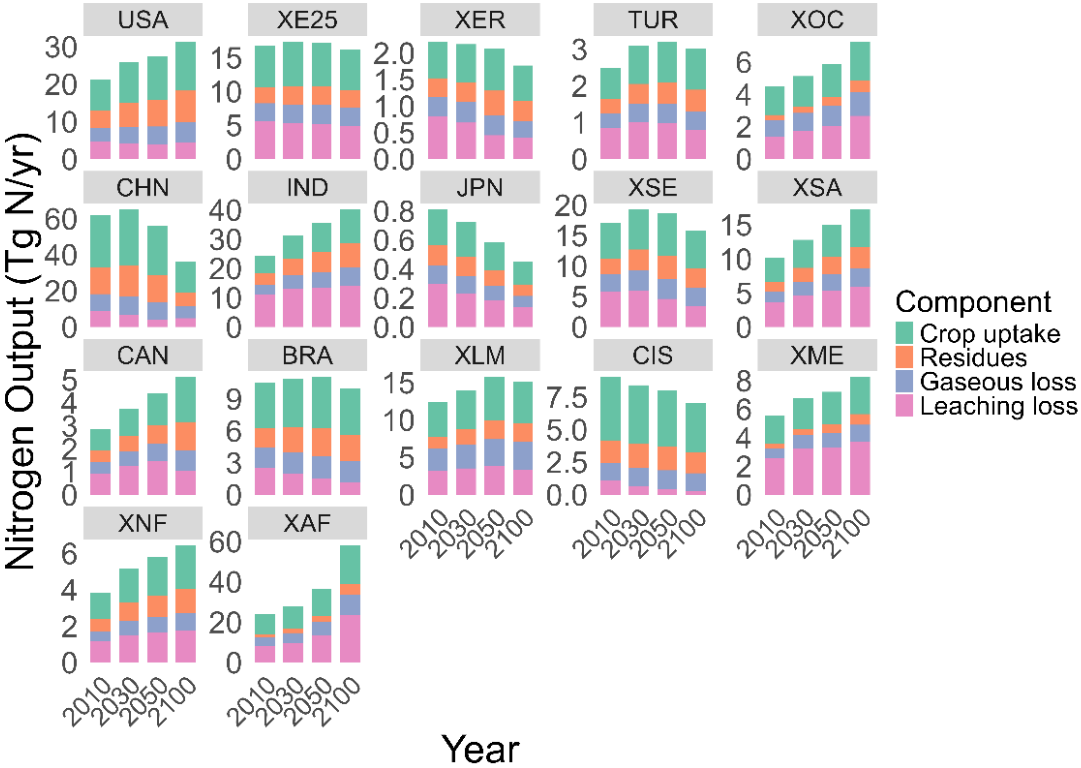

Figure 8 Temporal changes in nitrogen outputs from agricultural land by region (500C)

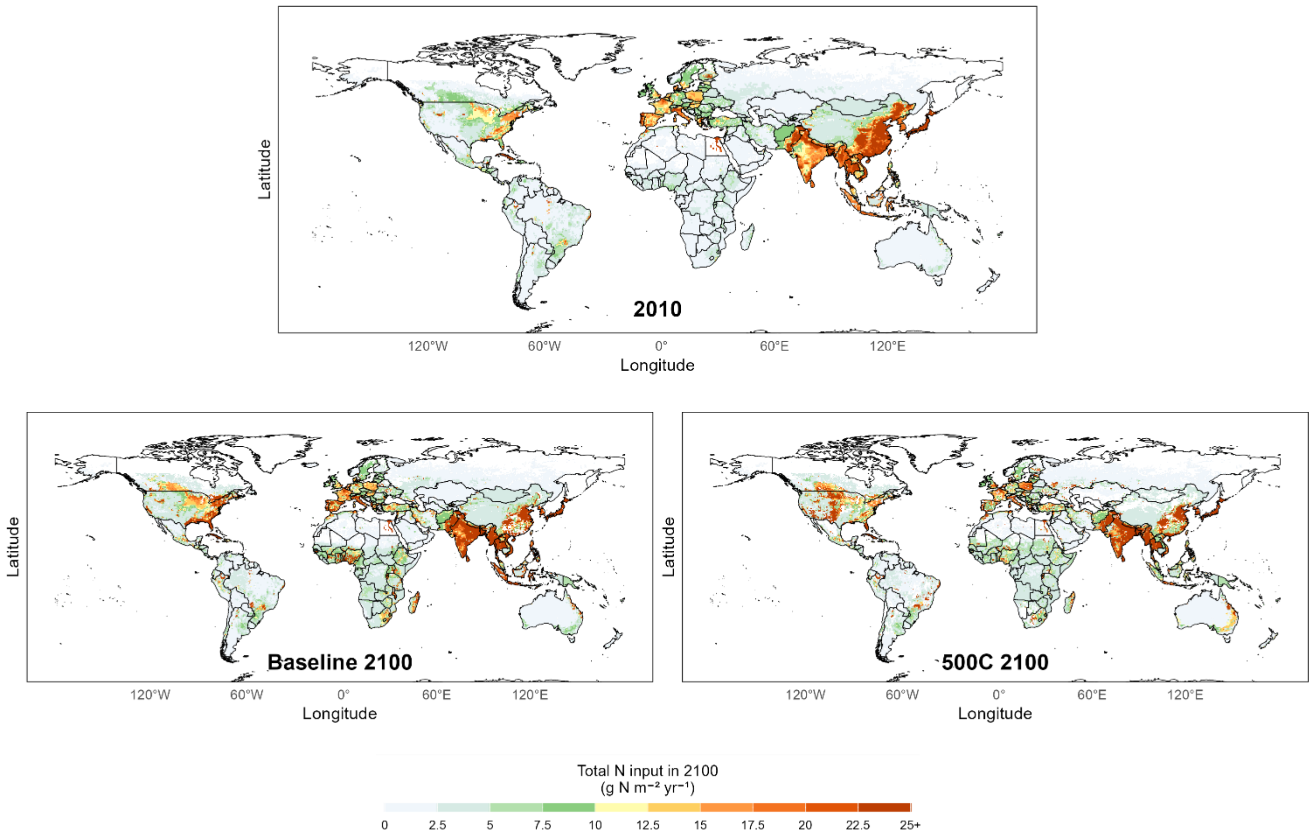

Figure 9 Nitrogen input per unit area of agricultural land worldwide (2010, Baseline 2100, and 500C scenario 2100)

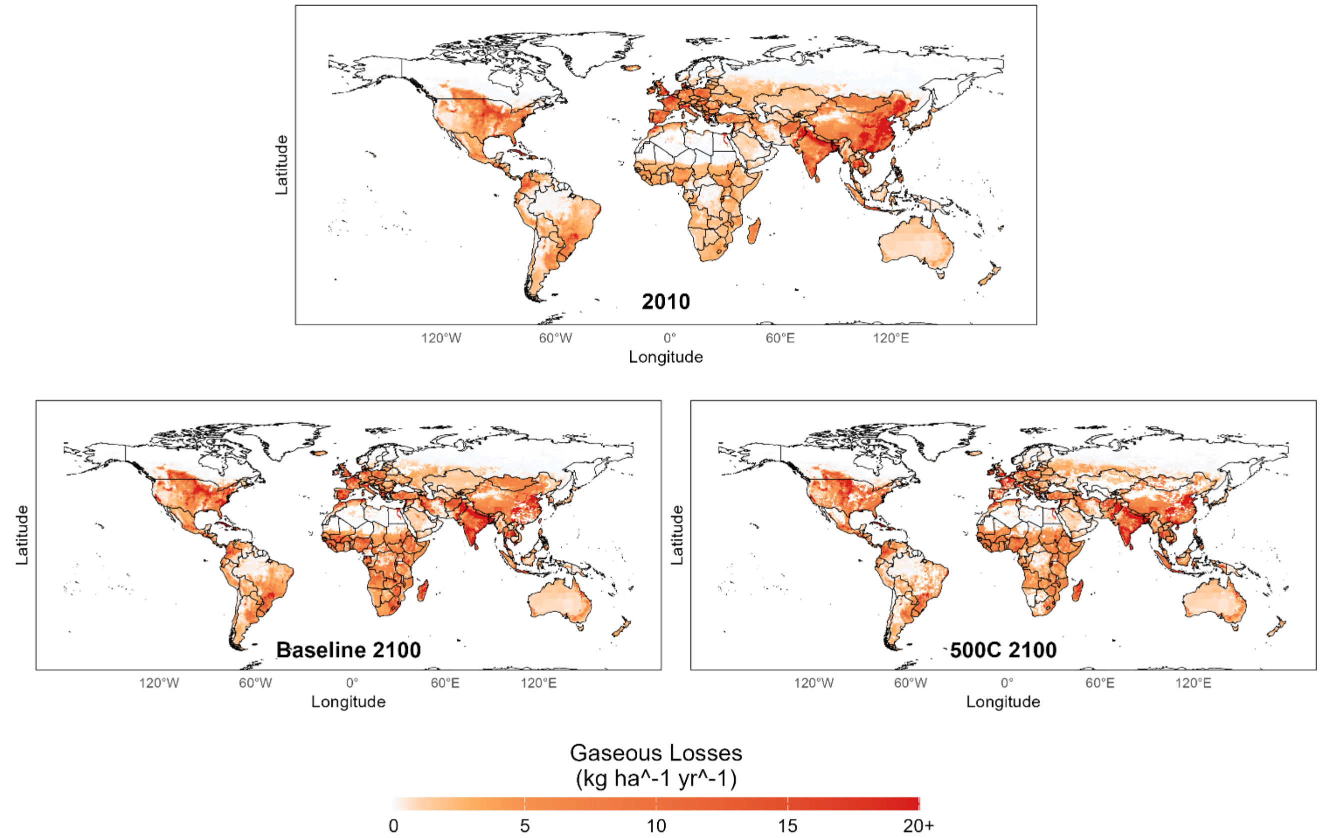

Figure 10 Nitrogen flux emitted as gases from agricultural land (2010, Baseline 2100, and 500C scenario 2100)

3.3 Distribution of nitrogen inputs and outputs to agricultural land

Nitrogen inputs to agricultural land worldwide, defined as $IN_{fer} + IN_{man} + IN_{dep} + IN_{fix}$, showed marked spatial heterogeneity. In 2010, high nitrogen inputs exceeding 20 g N m^{-2} yr^{-1} were concentrated in northern China and northern India, and similar patterns were also observed in Japan and parts of Southeast Asia (**Fig. 9**). Under the Baseline scenario in 2100, regions with high nitrogen input expanded mainly in India and Southeast Asia, whereas in some parts of China the input per unit area decreased because agricultural land expanded substantially relative to the increase in total nitrogen input. Under the 500C scenario, nitrogen inputs increased in Africa and India, but the increase in Africa was smaller than under the Baseline scenario, and in North America the high-input areas shifted from the eastern part of the continent toward the central region.

The spatial distribution of gaseous nitrogen emissions from agricultural land also exhibited clear regional patterns (**Fig. 10**). In 2010, emissions exceeding 20 kg N ha^{-1} yr^{-1} were found in parts of China and India. Under the Baseline scenario in 2100, regions with high emissions expanded in India and Africa. Although the overall pattern under the 500C scenario was similar to that under the Baseline scenario, some differences were observed, such as a shift of the emission hotspot in North America toward the central region.

4. Discussion

4.1 Interpretation

In this study, we developed a grid-based terrestrial nitrogen flow model within the integrated assessment framework of AIM to represent nitrogen inputs to agricultural land, recovery as crops and crop residues, gaseous emissions, and leaching to soils and water bodies, and examined its validity through comparison with existing emission inventories and previous studies. Specifically, we compared agricultural soil emissions of NO_x, NH_3, and N_2O in 2010 with those in AIM-Hub, EDGAR, CEDS, and FAOSTAT, and also compared nitrogen leaching from agricultural land to soils and water bodies with previous estimates, in order to evaluate how well the model reproduces plausible nitrogen flows at the global scale. In doing so, this study presented a method for spatially explicit representation of agricultural nitrogen flows within the AIM integrated assessment framework and demonstrated its applicability.

As shown in **Table 1**, the agricultural soil emissions of NO_x, NH_3, and N_2O estimated by the present model were generally consistent with existing emission inventories, suggesting that the model has a certain degree of validity for use in global-scale assessments. Compared with AIM-Hub, the present model estimated agricultural soil NH_3 emissions to be 6.9 Tg N yr^{-1} lower, whereas total agricultural-sector NH_3 emissions shown in **Table 1** were 13.4 Tg N yr^{-1} higher in the present model. This difference is likely attributable to differences in the treatment of NH_3 volatilized directly to the atmosphere from livestock excreta remaining on agricultural land. In the present model, such emissions are not included in agricultural soil emissions, but are instead counted separately as volatilization during the manure management process. In contrast, AIM-Hub includes similar emissions in its estimates of agricultural soil emissions. In addition, **Table 1** shows that the differences of emission in agricultural sector between AIM-Hub and EDGAR are less than 1.7 Tg N yr^{-1} for all three chemical species, which is likely because AIM-Hub is calibrated based on EDGAR estimates.

A comparison of regional agricultural soil NH_3 emissions in 2010 with AIM-Hub, as shown in **Fig. 2**, indicates that the estimates were similar in many regions, whereas the present model produced higher estimates than AIM-Hub in sub-Saharan Africa and the rest of Asia. In the present study, IN_{fer} and IN_{man} were used as explanatory variables in addition to soil conditions in estimating emissions. Because IN_{fer} in 2010 is consistent with AIM-Hub, the larger discrepancies in sub-Saharan Africa and the rest of Asia are likely attributable to the greater contribution of IN_{man} in those regions, as shown in **Fig. 5**.

On the other hand, the terrestrial nitrogen flow model developed in this study estimated nitrogen leaching from agricultural land to soils and water bodies to be larger than the estimates of Bouwman et al. (2005), Beusen et al. (2022), and related studies. One possible reason for this difference, shown in **Table 2**, is that the present study considers the process by which crop residues are reused as fertilizer, whereas this process is not necessarily included in other models. Another factor is the uncertainty in the exogenous data used both in this model and in previous studies. In addition, Smil (1999), Beusen et al. (2022), and Liu et al. (2010) include, in the total nitrogen loss from agricultural land, nitrogen flows other than gaseous emissions and leaching, such as nitrogen lost through erosion. As a result, their estimates of leaching may have been relatively smaller. In contrast, the present study does not include erosion in outputs from agricultural land, because nitrogen transported by erosion does not necessarily flow out of the grid.

Previous studies on nitrogen leaching are limited, and even in those studies, leaching estimates are based on limited observations and thus involve substantial uncertainty, as in the present model (Bouwman et al., 2005; Smil, 1999). Considering both the magnitude of this uncertainty and the differences in the definition of OUT_{lea} discussed above, the differences in leaching estimates between this study and previous studies shown in **Table 2** do not necessarily undermine the validity of the terrestrial nitrogen flow model developed in this study. Nevertheless, there remains room for further improvement of the model in the future through refinement of the formulation of the leaching process and comparison with observational data.

As shown in **Fig. 4**, one possible reason why IN_{fer} increased after 2030 under each scenario is the increase in global cropland area in the AIM-PLUM output. In addition, one of the factors behind the smaller increase in IN_{fer} under the 500C scenario than under the Baseline scenario is that the expansion of cropland area was more constrained than in the Baseline scenario. Furthermore, whereas cropland area increased by about 24.7% from 2010 to 2100 in the Baseline scenario, IN_{fer} increased by about 41.3%, suggesting that not only the expansion of cropland area but also the increase in synthetic fertilizer input per unit cropland area contributed to the increase in IN_{fer}. In this study, future changes in agricultural land area and synthetic fertilizer input were based on the output of the integrated assessment model AIM-Hub. In AIM-Hub, crop demand and land demand are estimated through an optimization process that considers multiple economic factors, including crop prices, agricultural land prices, and policy constraints for greenhouse gas mitigation. Under the Baseline scenario, increasing crop demand associated with economic growth and population growth promotes agricultural land expansion. By contrast, under the 500C scenario, activity levels in all sectors, including agriculture, are relatively constrained under stringent greenhouse gas emission limits, and land demand is therefore also limited, resulting in a tendency for agricultural land expansion to be suppressed. In addition, AIM-Hub uses a mainly emission factor-based approach for projecting future synthetic fertilizer input to agricultural land, in which the temporal rate of change in N_2O emissions—estimated by multiplying activity levels in each country by emission factors—is used as the rate of change in fertilizer input. Therefore, if activity levels are constrained, synthetic fertilizer input is also constrained accordingly. Although neither the present model nor AIM-Hub includes a parameter that directly controls synthetic fertilizer input per unit cropland area, the results show that under the 500C scenario the reduction in synthetic fertilizer input is larger than the reduction in cropland area, leading to a relative suppression of synthetic fertilizer input per unit cropland area. In addition, pastureland area also tends to increase after 2030 in the Baseline scenario, as does cropland area; however, because approximately 95% of synthetic fertilizer is assumed to be applied to cropland, the effect of increasing pastureland area on the temporal change in IN_{fer} is considered to be limited.

Likewise, the large increase in IN_{man} after 2030 under each scenario (**Fig. 4**) is attributable to the substantial increase in global livestock production. In this study, the amount of manure changes linearly with livestock production estimated by AIM-Hub; therefore, livestock production increased under each scenario, and IN_{man} increased accordingly.

Under both the Baseline and 500C scenarios, OUT_{crop} showed the largest increase over time among the output terms (**Fig. 4**), which is attributable to the increase in global crop demand and livestock production, because pasture consumed by livestock is also included in OUT_{crop}.

Furthermore, global nitrogen use efficiency was higher under the 500C scenario than under the Baseline scenario in every target year (**Fig. 4**), suggesting that climate change mitigation measures may provide a co-benefit in terms of nitrogen use efficiency. However, even the amount of nitrogen lost from agricultural soils to the environment ($OUT_{gas} + OUT_{lea}$, excluding volatilization from manure management systems) exceeded 100 Tg N yr^{-1} in all scenarios and target years. Considering that the Planetary Boundaries framework (De Vries et al., 2013) proposes a global threshold of 82 Tg N yr^{-1} for anthropogenic nitrogen fixation, these results suggest that the co-benefits of climate change mitigation alone are insufficient, and that much larger reductions in nitrogen inputs and improvements in nitrogen use efficiency are still required.

As shown in **Fig. 5**, nitrogen inputs to agricultural land increased consistently from 2010 to 2100 in Africa, India, the Middle East, South America, and North America, where future population growth is expected. In these regions, expansion of cultivated area and intensification are likely to progress in response to growing demand for food, including cereals and livestock products, resulting in increases in IN_{fer} and IN_{man}. In particular, because the contribution of IN_{man} is relatively large in regions such as sub-Saharan Africa, the impact of increasing livestock numbers on nitrogen flows is suggested to be substantial. In contrast, in regions such as China and Japan, where activity levels are projected to decline in AIM-Hub, IN_{fer} and IN_{man} decrease, and total nitrogen inputs also decline over time. Because IN_{dep} and IN_{fix} account for only a small share of total inputs and show limited temporal variation, the future changes in nitrogen flows in agricultural land are mainly driven by fertilizer input and livestock production.

The temporal change in OUT_{crop} (**Fig. 6**) corresponds to the change in crop yield estimated by AIM-Hub, and OUT_{res} also changes in a broadly similar manner. However, because OUT_{crop} includes nitrogen in pasture consumed by livestock and OUT_{res} is considered only for cropland, the relationship is not simply linear. In particular, in sub-Saharan Africa and other pasture-dominated regions, the contribution of OUT_{res} is smaller relative to OUT_{crop}. In addition, because OUT_{lea} is calculated as the difference between total inputs and OUT_{crop}, OUT_{res}, and OUT_{gas}, any changes in the input side and in OUT_{crop}, OUT_{res}, and OUT_{gas} are fully absorbed by OUT_{lea}. As a result, the variability of OUT_{lea} becomes relatively large in most regions.

Figure 9 shows that, in 2010, nitrogen input per unit area was large in regions with high agricultural intensity and high fertilizer application, such as China, India, Japan, the United States, and Europe. In these regions, high GDP and population density, together with strong food demand and a high dependence on intensive livestock production and chemical fertilizers, are considered to underlie the high input levels. Under the Baseline scenario in 2100, areas with high input expand in India, Southeast Asia, and parts of Africa, suggesting that hotspots of nitrogen loading may spread toward the Global South as food demand increases in emerging and developing countries. On the other hand, in some parts of China, input per unit area declines because of the expansion of agricultural land area, suggesting that an increase in production does not necessarily imply an increase in local nitrogen loading. Under the 500C scenario, nitrogen inputs increase in Africa and India as well, but the magnitude of increase is smaller than under the Baseline scenario, indicating that the introduction of climate change mitigation measures may contribute to constraining nitrogen inputs over the long term.

Figure 10 broadly corresponds to the distribution of inputs and clearly shows that grids with larger nitrogen inputs also tend to have larger gaseous emissions. This is attributable to the fact that fertilizer input is included as one of the major determinants in the equation used to estimate gaseous nitrogen emissions in the terrestrial nitrogen flow model developed in this study (Eq. 14).

4.2 Future challenges

This section discusses the limitations of the estimates presented in this study. First, one limitation lies in the linearity of land-use determination in AIM-PLUM, the land-use allocation model. Under the current modeling framework, changes in land demand may induce unrealistic responses in land-use change. Second, the coarse regional classification and crop classification used in this study also represent important challenges. Compared with methods based on country-level estimation, the approach adopted here is more likely to reflect differences in drivers among grids. As a result, however, the terrestrial nitrogen flow model developed in this study is more prone to spatial bias arising from the coarse regional classification. In addition, the coarse crop classification increases the uncertainty of the parameters used to estimate the amount of nitrogen contained in crops and crop residues. If a finer crop classification, comparable to that used in GAEZ (Global Agro-Ecological Zones), were available, OUT_{crop} and OUT_{res} could be estimated directly by multiplying yieldgrid by crop-specific nitrogen contents. In that case, the weighting procedure based on global crop production data from FAOSTAT could be omitted, which might reduce uncertainty. Furthermore, another limitation is that the target years do not match in the comparison between estimated and observed values of nitrogen loading to rivers. As shown by Nishina et al. (2021), nitrogen runoff through rivers changed by several percent in some basins between the 1990s and 2010, and such temporal changes may have affected the differences between estimates and observations. Nevertheless, although a certain degree of uncertainty remains, this issue is not considered large enough to substantially undermine the validity of the model from the perspective of river-specific nitrogen loading.

5. Conclusion

In this study, we newly developed a grid-based terrestrial nitrogen flow model that can be linked with the AIM framework and examined its validity. We also assessed, at the global scale, the impacts of land-use changes associated with climate change mitigation on nitrogen flows in agricultural land and nitrogen loading to rivers. Specifically, nitrogen flows were quantified on a 0.5° × 0.5° grid, with synthetic fertilizer, manure, atmospheric deposition, and biological nitrogen fixation treated as inputs, and nitrogen recovery in crops and residues, gaseous emissions to the atmosphere (e.g., NO_x, NH_3, and N_2O), and leaching to soils and water bodies treated as outputs.

The terrestrial nitrogen flow model developed in this study estimated agricultural soil emissions of NH_3, NO_x, and N_2O in the base year 2010 at levels comparable to those reported in existing global inventories such as EDGAR, FAOSTAT, and AIM-Hub. On the other hand, nitrogen leaching from agricultural land to soils and water bodies was estimated to be larger than in previous studies, which is likely attributable to differences in the treatment of crop residue recycling, the definition of nitrogen flows including leaching and erosion, and parameter uncertainty.

In addition, under the 500C scenario, nitrogen inputs to agricultural land and gaseous emissions were lower than under the Baseline scenario, while nitrogen use efficiency remained relatively higher. These results suggest that climate change mitigation measures may provide co-benefits not only through reducing greenhouse gas emissions but also through suppressing nitrogen emissions from agricultural land.

The nitrogen flow model developed in this study, as well as the broader framework that incorporates it, provides a foundation for conducting grid-based research across a wide range of fields, including climate change, nitrogen cycling, atmospheric chemistry, and land use.

Acknowledgements

This study was supported by the Japan Science and Technology Agency (JST) as part of the Adopting Sustainable Partnerships for Innovative Research Ecosystem (ASPIRE) program (Grant Number JPMJAP2331), the Environment Research and Technology Development Fund (JPMEERF20241001) of the Environmental Restoration and Conservation Agency provided by the Ministry of the Environment of Japan, and the Sumitomo Electric Industries Group CSR Foundation.

References

Beusen, A. H. W., Doelman, J. C., Van Beek, L. P. H., Van Puijenbroek, P. J. T. M., Mogollón, J. M., Van Grinsven, H. J. M., Stehfest, E., Van Vuuren, D. P., and Bouwman, A. F.: Exploring river nitrogen and phosphorus loading and export to global coastal waters in the Shared Socio-economic pathways, Global Environmental Change, 72, 102426, https://doi.org/10.1016/j.gloenvcha.2021.102426, 2022.

Bey, I., Jacob, D. J., Yantosca, R. M., Logan, J. A., Field, B. D., Fiore, A. M., Li, Q., Liu, H. Y., Mickley, L. J., and Schultz, M. G.: Global modeling of tropospheric chemistry with assimilated meteorology: Model description and evaluation, J. Geophys. Res., 106, 23073–23095, https://doi.org/10.1029/2001JD000807, 2001.

Bosilovich, M. G., Lucchesi, R., & Suarez, M., MERRA-2: File Specification, 2015.

Bouwman, A. F., Lee, D. S., Asman, W. A. H., Dentener, F. J., Van Der Hoek, K. W., and Olivier, J. G. J.: A global high‐resolution emission inventory for ammonia, Global Biogeochemical Cycles, 11, 561‐587, https://doi.org/10.1029/97GB02266, 1997.

Bouwman, A. F., Van Drecht, G., and van der Hoek, K. W.: Surface N balances and reactive N loss to the environment from global intensive agricultural production systems for the period 1970–2030, Sci. China Ser. C.-Life Sci., 48, 767–779, https://doi.org/10.1007/BF03187117, 2005.

Bouwman, L., Goldewijk, K. K., Van Der Hoek, K. W., Beusen, A. H. W., Van Vuuren, D. P., Willems, J., Rufino, M. C., and Stehfest, E.: Exploring global changes in nitrogen and phosphorus cycles in agriculture induced by livestock production over the 1900–2050 period, Proc. Natl. Acad. Sci. U.S.A., 110, 20882–20887, https://doi.org/10.1073/pnas.1012878108, 2013.

Crippa, M., Guizzardi, D., Muntean, M., Schaaf, E., Dentener, F., Van Aardenne, J. A., Monni, S., Doering, U., Olivier, J. G. J., Pagliari, V., and Janssens-Maenhout, G.: Gridded emissions of air pollutants for the period 1970–2012 within EDGAR v4.3.2, Earth Syst. Sci. Data, 10, 1987–2013, https://doi.org/10.5194/essd-10-1987-2018, 2018.

De Vries, W., Kros, J., Kroeze, C., and Seitzinger, S. P.: Assessing planetary and regional nitrogen boundaries related to food security and adverse environmental impacts, Current Opinion in Environmental Sustainability, 5, 392–402, https://doi.org/10.1016/j.cosust.2013.07.004, 2013.

Dodds, W. K.: Nutrients and the “dead zone”: the link between nutrient ratios and dissolved oxygen in the northern Gulf of Mexico, Frontiers in Ecology and the Environment, 4, 211–217, https://doi.org/10.1890/1540-9295(2006)004%255B0211:NATDZT%255D2.0.CO;2, 2006.

Fowler, D., Coyle, M., Skiba, U., Sutton, M. A., Cape, J. N., Reis, S., Sheppard, L. J., Jenkins, A., Grizzetti, B., Galloway, J. N., Vitousek, P., Leach, A., Bouwman, A. F., Butterbach-Bahl, K., Dentener, F., Stevenson, D., Amann, M., and Voss, M.: The global nitrogen cycle in the twenty-first century, Philosophical Transactions of the Royal Society B: Biological Sciences, https://doi.org/10.1098/rstb.2013.0164, 2013.

FAOSTAT: Fertilizers by Product., https://www.fao.org/faostat/en/#data/RFB, Accessed on 13 January 2026.

Fujimori, S., Masui, T., & Matsuoka, Y.: AIM/CGE V2.0 Model Formula, In S. Fujimori, M. Kainuma, & T. Masui (Eds.), Post-2020 Climate Action: Global and Asian Perspectives, Springer, 201–303., 2017a.

Fujimori, S., Abe, M., Kinoshita, T., Hasegawa, T., Kawase, H., Kushida, K., Masui, T., Oka, K., Shiogama, H., Takahashi, K., Tatebe, H., and Yoshikawa, M.: Downscaling Global Emissions and Its Implications Derived from Climate Model Experiments, PLoS ONE, 12, e0169733, https://doi.org/10.1371/journal.pone.0169733, 2017b.

Galloway, J. N., Aber, J. D., Erisman, J. W., Seitzinger, S. P., Howarth, R. W., Cowling, E. B., and Cosby, B. J.: The Nitrogen Cascade, BioScience, 53, 341, https://doi.org/10.1641/0006-3568(2003)053%255B0341:TNC%255D2.0.CO;2, 2003.

Hasegawa, T., Fujimori, S., Ito, A., Takahashi, K., and Masui, T.: Global land-use allocation model linked to an integrated assessment model, Science of The Total Environment, 580, 787–796, https://doi.org/10.1016/j.scitotenv.2016.12.025, 2017.

Hoesly, R. M., Smith, S. J., Feng, L., Klimont, Z., Janssens-Maenhout, G., Pitkanen, T., Seibert, J. J., Vu, L., Andres, R. J., Bolt, R. M., Bond, T. C., Dawidowski, L., Kholod, N., Kurokawa, J., Li, M., Liu, L., Lu, Z., Moura, M. C. P., O’Rourke, P. R., and Zhang, Q.: Historical (1750–2014) anthropogenic emissions of reactive gases and aerosols from the Community Emissions Data System (CEDS), Geosci. Model Dev., 11, 369–408, https://doi.org/10.5194/gmd-11-369-2018, 2018.

Hongmin, D., Joe, M., Tim., A., M., Jerry., L., H., Don-ald., E., J., Keith., R., L., Magda., A., L., Anna., R.: EMISSIONS FROM LIVESTOCK AND MANURE MANAGEMENT, 2006 IPCC Guidelines for National Greenhouse Gas Inventories, 2006.

IFASTAT: Fertilizer Use By Crop, https://www.ifastat.org/consumption/fertilizer-use-by-crop, Accessed on 13 January 2026.

King, G., Honaker, J., Joseph, A., and Scheve, K.: Analyzing Incomplete Political Science Data: An Alternative Algorithm for Multiple Imputation, Am Polit Sci Rev, 95, 49–69, https://doi.org/10.1017/S0003055401000235, 2001.

Lassaletta, L., Billen, G., Garnier, J., Bouwman, L., Velazquez, E., Mueller, N. D., and Gerber, J. S.: Nitrogen use in the global food system: past trends and future trajectories of agronomic performance, pollution, trade, and dietary demand, Environ. Res. Lett., 11, 095007, https://doi.org/10.1088/1748-9326/11/9/095007, 2016.

Lesschen, J. P., Stoorvogel, J. J., and Smaling, E.: Scaling soil nutrient balances: enabling mesolevel applications for African realities, Food and Agriculture Organization of the United Nations, Rome, 132 pp., 2004.

Liu, J., You, L., Amini, M., Obersteiner, M., Herrero, M., Zehnder, A. J. B., and Yang, H.: A high-resolution assessment on global nitrogen flows in cropland, Proc. Natl. Acad. Sci. U.S.A., 107, 8035–8040, https://doi.org/10.1073/pnas.0913658107, 2010.

Milbrandt, A.: A Geographic Perspective on the Current Biomass Resource Availability in the United States, Technical Report, 2005.

Nishina, K., Ito, A., Hanasaki, N., and Hayashi, S.: Reconstruction of spatially detailed global map of NH4+ and NO3− application in synthetic nitrogen fertilizer, Earth System Science Data, 9, 149–162, https://doi.org/10.5194/essd-9-149-2017, 2017.

Nishina, K., Ito, A., Zhou, F., Yan, X., Hayashi, S., and Winiwarter, W.: Historical trends of riverine nitrogen loading from land to the East China Sea: a model-based evaluation, Environ. Res. Commun., 3, 085005, https://doi.org/10.1088/2515-7620/ac1ce8, 2021.

Popp, A., Calvin, K., Fujimori, S., Havlik, P., Humpenöder, F., Stehfest, E., Bodirsky, B. L., Dietrich, J. P., Doelmann, J. C., Gusti, M., Hasegawa, T., Kyle, P., Obersteiner, M., Tabeau, A., Takahashi, K., Valin, H., Waldhoff, S., Weindl, I., Wise, M., Kriegler, E., Lotze-Campen, H., Fricko, O., Riahi, K., and Vuuren, D. P. V.: Land-use futures in the shared socio-economic pathways, Global Environmental Change, 42, 331–345, https://doi.org/10.1016/j.gloenvcha.2016.10.002, 2017.

Sanderman, J., Woolf, D., Lehmann, J., Rivard, C., Poggio, L., Heuvelink, G., and Bossio, D.: Soils Revealed soil carbon futures (3.0), https://doi.org/10.7910/DVN/HA17D3, 2020.

Riahi, K., Bertram, C., Huppmann, D., Rogelj, J., Bosetti, V., Cabardos, A.-M., Deppermann, A., Drouet, L., Frank, S., Fricko, O., Fujimori, S., Harmsen, M., Hasegawa, T., Krey, V., Luderer, G., Paroussos, L., Schaeffer, R., Weitzel, M., Van Der Zwaan, B., Vrontisi, Z., Longa, F. D., Després, J., Fosse, F., Fragkiadakis, K., Gusti, M., Humpenöder, F., Keramidas, K., Kishimoto, P., Kriegler, E., Meinshausen, M., Nogueira, L. P., Oshiro, K., Popp, A., Rochedo, P. R. R., Ünlü, G., Van Ruijven, B., Takakura, J., Tavoni, M., Van Vuuren, D., and Zakeri, B.: Cost and attainability of meeting stringent climate targets without overshoot,

Nat. Clim. Chang., 11, 1063–1069, https://doi.org/10.1038/s41558-021-01215-2, 2021.
Smil, V.: Nitrogen in crop production: An account of global flows, Global Biogeochemical Cycles, 13, 647–662, https://doi.org/10.1029/1999GB900015, 1999.
Stehfest, E. and Bouwman, L.: N2O and NO emission from agricultural fields and soils under natural vegetation: summarizing available measurement data and modeling of global annual emissions, Nutr Cycl Agroecosyst, 74, 207–228, https://doi.org/10.1007/s10705-006-9000-7, 2006.
Stewart, W. M. and Roberts, T. L.: Food Security and the Role of Fertilizer in Supporting it, Procedia Engineering, 46, 76–82, https://doi.org/10.1016/j.proeng.2012.09.448, 2012.
Tilman, D.: Global environmental impacts of agricultural expansion: The need for sustainable and efficient practices, Proceedings of the National Academy of Sciences, 96(11), 5995–6000, 1999.

Key Words：Nitrogen cycle，Reactive nitrogen，Atmospheric chemistry，Chemical Transport Model